ACS Infectious Diseases

Article

Binding Mode Characterization and Early in vivo Evaluation of Fragment-like Thiols as Inhibitors of the Virulence Factor LasB from Pseudomonas aeruginosa

Andreas Martin Kany, Asfandyar Sikandar, Jörg Haupenthal, Samir Yahiaoui, Christine K. Maurer, Ewgenij Proschak, Jesko Koehnke, and Rolf W. Hartmann

ACS Infect. Dis., **Just Accepted Manuscript** • DOI: 10.1021/acsinfecdis.8b00010 • Publication Date (Web): 27 Feb 2018

ACS Publications

ACS Infectious Diseases is published by the American Chemical Society. 1155 Sixteenth Street N.W., Washington, DC 20036

Binding Mode Characterization and Early *in vivo* Evaluation of Fragment-like Thiols as Inhibitors of the Virulence Factor LasB from *Pseudomonas aeruginosa*

Andreas M. Kany,[†,⊥] Asfandyar Sikandar,[‡,⊥] Jörg Haupenthal,[†] Samir Yahiaoui,[†] Christine K. Maurer,[†] Ewgenij Proschak,[ǁ] Jesko Köhnke,[‡] Rolf W. Hartmann[*,†,§]

[†] Helmholtz Institute for Pharmaceutical Research Saarland (HIPS), Department of Drug Design and Optimization, Campus E8.1, 66123, Saarbrücken, Germany

[‡] Helmholtz Institute for Pharmaceutical Research Saarland (HIPS), Workgroup Structural Biology of Biosynthetic Enzymes, Campus E8.1, 66123, Saarbrücken, Germany

[§] Department of Pharmacy, Pharmaceutical and Medicinal Chemistry, Saarland University, Campus E8.1, 66123 Saarbrücken, Germany

[ǁ] Institute of Pharmaceutical Chemistry, Goethe University Frankfurt, Max-von-Laue-Straße 9, 60438 Frankfurt, Germany

***** Rolf.Hartmann@helmholtz-hzi.de

The increasing emergence of antibiotic resistance necessitates the development of anti-infectives with novel modes of action. Targeting bacterial virulence is considered a promising approach to develop novel antibiotics with reduced selection pressure. The extracellular collagenase elastase (LasB) plays a pivotal role in the infection process of *Pseudomonas aeruginosa* and therefore represents an attractive anti-virulence target. Mercaptoacetamide-based thiols have been reported to inhibit LasB as well as collagenases from clostridia and bacillus species. The present work provides an insight into the Structure-Activity-Relationship (SAR) of these fragment-like LasB inhibitors, demonstrating an inverse activity profile compared to similar inhibitors of clostridial collagenase H (ColH). An X-ray co-crystal structure is presented, revealing distinct binding of two compounds to the active site of LasB, which unexpectedly maintains an open conformation. We further demonstrate *in vivo* efficacy in a *Galleria mellonella* infection model and high selectivity of the LasB inhibitors toward human matrix-metalloproteinases (MMPs).

Keywords: antibiotic resistance, anti-virulence agent, elastase, LasB, binding mode, selectivity, *Galleria mellonella*

The increasing emergence of resistant bacteria poses a threat to public health, especially in case of Gram-negative species.[1,2] *Pseudomonas aeruginosa* is one of the three most problematic pathogens on

the WHO priority list.[1] It is the reason for many hospital-acquired infections as well as fatal lung infections in cystic fibrosis and bronchiectasis patients.[3,4] To combat the rise of antibiotic-resistant *Pseudomonas aeruginosa* infections, novel treatment options are urgently needed.[5,6]

A promising new approach to reduce selection pressure is to target bacterial virulence in order to disarm pathogens rather than to kill them.[7–10] *Pseudomonas aeruginosa* produces numerous virulence factors contributing to disease progression, which provide attractive anti-infective targets.[11–14] The secreted enzyme LasB is a major virulence factor, playing a crucial role for the pathogenicity of *P. aeruginosa*.[15] The enzyme is a zinc-metalloprotease with high structural similarity to thermolysin.[16,17] One of its main functions is the cleavage of components of the connective tissue like elastin[15] or collagen[18] to allow the bacteria to colonize a niche in the host. Tissue damage is further caused by disruption of cell-to-cell junctions.[19,20] Additionally, LasB enables *P. aeruginosa* to evade the human immune response by cleaving i.a. IgG[21], cytokines[22], surfactant proteins A and D[23], complement factor C3[24] or pulmonary defense receptor PAR2.[25] Consequently, this protease represents an attractive anti-infective target and its extracellular localization facilitates drug discovery as permeation of the Gram-negative cell wall is not needed.[9,26]

LasB belongs to the thermolysin (M4) family of enzymes.[27] For this class it has been reported that the rather open active site cleft of the protease adopts a more closed conformation upon inhibitor binding.[28] To date, several zinc-chelating inhibitors of LasB have been described,[29–32] including compounds bearing a mercaptoacetamide motif attached either to small peptides[33] or to aniline.[34] Crystallographic data shedding light on the binding mode of these thiols to the protease has not been available yet. We have recently described *N*-aryl mercaptoacetamide-based compounds as very potent clostridial collagenase inhibitors with high selectivity toward human matrix metalloproteinases (MMPs).[35] The compounds contain a prodrug-like thiocarbamate-motif, which liberates free thiols as active form after hydrolysis in buffer. The best ColH inhibitor **1** (Figure 1) was also found to inhibit LasB.

In this work, we report a functional screening followed by LC-MS validation for LasB inhibition of the focused TimTec ActiTarg-P library previously used to discover the ColH inhibitors. The only inhibitor resulting from the screening was an *N*-aryl mercaptoacetamide. Encouraged by the promising inhibitory activity and selectivity, we wanted to gain further insight into LasB inhibition by this compound class. We describe the activity and selectivity profiles of a broad range of *N*-aryl mercaptoacetamides. An X-ray crystal structure of a mercaptoacetamide-based inhibitor in complex with LasB is presented revealing an unprecedented open conformation of the active site, which harbors two inhibitor molecules. To the best of our knowledge, this is the first description of inhibitor binding to LasB which does not lead to a closure of the active site cleft.

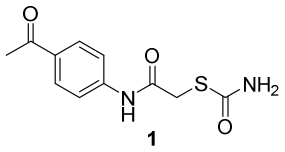

1

Figure 1. Structure of most potent ColH inhibitor **1.**

RESULTS AND DISCUSSION

Screening for Novel LasB Inhibitors.

In order to expand the chemical space of LasB inhibitors, we performed a functional screening based on the FRET-based *in vitro* assay developed by Nishino and Powers.[36] We used a protease inhibitor-enriched library which, after removing structures known as PAINS[37], comprised 1192 low molecular weight compounds. In addition, we included 330 fragments (Maybridge Fragment Library) into the screening. The only compound showing more than 50% inhibition when tested at 100 µM was mercaptoacetamide **2 (**Figure 2**).** Several false-positive hits had to be excluded because of quenching of substrate fluorescence.

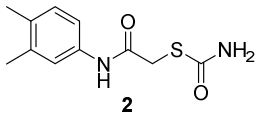

2

Figure 2. Structure of screening hit **2**.

Development of an LC-MS-based Readout for the FRET Assay.

In the FRET-based proteolytic assay, active LasB cleaves a quenched substrate, which results in an increase of fluorescence.[36] Enzyme inhibition leads to reduced substrate cleavage and consequently to reduced fluorescence. However, compounds interfering with the fluorophore by quenching effects[38] can pretend enzyme inhibition, resulting in false-positive hits.[39,40] Several quenching compounds were found, especially among fragments. To clarify if reduced fluorescence was caused by protease inhibition or to quenching effects, we developed an LC-MS-based readout for the FRET Assay. Elastase cleaves the synthetic substrate Abz-Ala-Gly-Leu-Ala-Nba (**3**) at the Gly-Leu bond[36,41], forming cleavage products **4** and **5** (Figure 3, A) which could be separated chromatographically. Using the published LasB inhibitor phosphoramidon[42] as a positive control, the FRET-assay results were excellently reproduced using an LC-MS-based readout which was based on the mass peak of cleavage product **5** (Figure S1). Applying this technology, we could detect several false positives whose apparent inhibition in the FRET assay was only due to quenching. Two examples are shown in Figure 3, B.

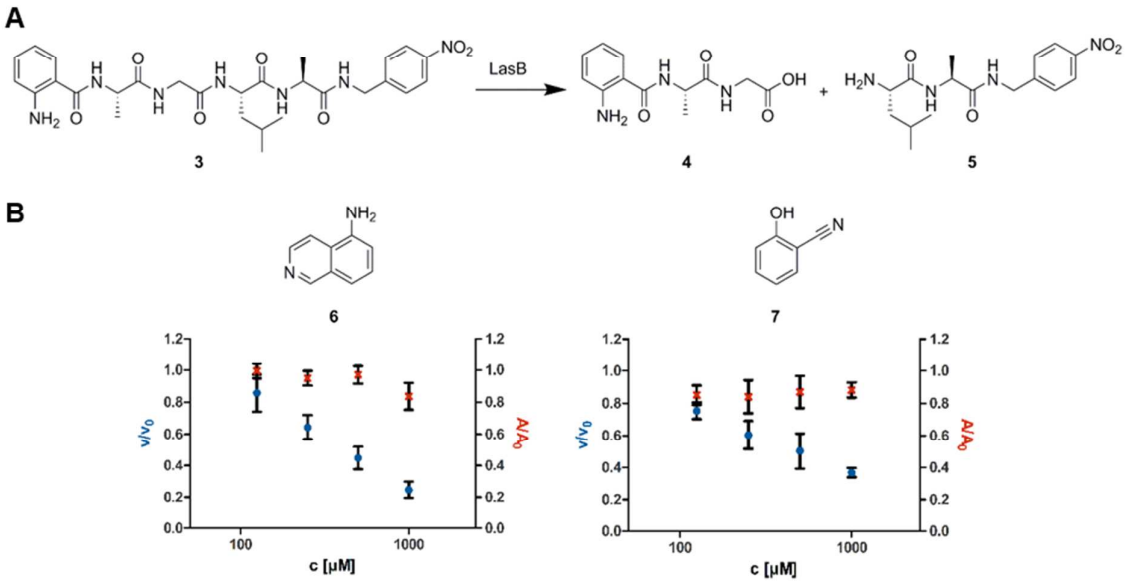

Figure 3. (A) Cleavage of FRET substrate Abz-Ala-Gly-Leu-Ala-Nba (**3**) into products **4** and **5** by LasB. Abz = 2-Aminobenzoyl; Nba = 4-nitrobenzylamide. (B) Structure and comparison of FRET (blue, v/v_0) vs. LC-MS results (red, A/A_0) for fragments **6** and **7**.

SAR of *N*-Aryl Mercaptoacetamides.

To elucidate the SAR of *N*-aryl mercaptoacetamides, 35 derivatives were purchased or synthesized (for further information see SI), and tested for LasB inhibition applying the FRET-based *in vitro* assay (Table 1 and Table S1). Nonpolar aromatic substituents, especially halogens, turned out to be favorable for activity while polar hydrogen-bond accepting moieties led to significantly reduced inhibition. For the *o-, m-* and *p*-Cl derivatives **9**, **12** and **17** as well as *m-* and *p*-CH_3 derivatives **13** and **21** no substantial effect of the substitution position on activity was found. The same holds true for the methoxy (**11**, **15**, **23**) and *o-*,*p*-phenyl (**10**, **18**) analogues. Introduction of a second substituent improved the IC_{50} at least twofold. Addition of methyl or chlorine substituents to **17** resulted in the best compounds **26, 27** and **28**, displaying IC_{50} values in the one-digit micromolar range. An exception is dimethoxy derivative **32**, which showed an activity similar to the mono-methoxy analogues **11**, **15** and **23**. In comparison to the initial screening hit **2**, the activity could be improved by more than 2.5-fold. Two examples showed that the introduction of a third substituent was not beneficial for inhibition: Introduction of a methyl group to compound **26** led to a twofold drop in activity (**34**), while no difference was observed between di- and tri-methyl derivatives **29** and **33**.

Table 1: Chemical structures and LasB inhibition of a series of *N*-aryl mercaptoacetamides.

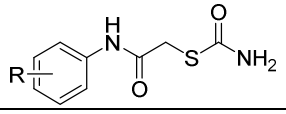

Cp.	R	IC_{50} (µM)	Cp.	R	IC_{50} (µM)	Cp.	R	IC_{50} (µM)
8	2-Br	11.4 ± 0.2	**17**	4-Cl	15.7 ± 0.4	**26**	2-CH_3-3-Cl	5.9 ± 0.3
9	2-Cl	14.1 ± 0.5	**18**	4-Ph	19.8 ± 1.4	**27**	3,4-di-Cl	6.2 ± 0.3
10	2-Ph	25.0 ± 0.8	**19**	4-Br	22.8 ± 1.1	**28**	2-CH_3-5-Cl	7.2 ± 0.2
11	2-OCH_3	51.7 ± 4.0	**20**	4-I	32.9 ± 1.3	**29**	2,4-di-CH_3	12.1 ± 0.4
12	3-Cl	19.4 ± 0.5	**21**	4-CH_3	36.1 ± 0.7	**30**	2,3-di-CH_3	12.3 ± 0.4
13	3-CH_3	47.5 ± 1.4	**22**	4-OC_2H_5	47.6 ± 1.1	**2**	3,4-di-CH_3	16.0 ± 1.9
14	3-F	59.2 ± 0.9	**23**	4-OCH_3	47.7 ± 1.0	**31**	3-Cl-4-CH_3	16.3 ± 1.0
15	3-OCH_3	61.7 ± 2.1	**1**	4-$COCH_3$	73.1 ± 2.5	**32**	2,4-di-OCH_3	54.0 ± 2.7
16	3-$NHSO_2CH_3$	127.2 ± 3.5	**24**	4-$COOCH_3$	81.5 ± 2.5	**33**[a]	2,4,6-tri-CH_3	11.9 ± 0.4
			25	4-(CH_2-1,2,4-triazole)	85.6 ± 2.3	**34**[a]	3-Cl-2,6-di-CH_3	11.9 ± 0.4

[a]Compounds **33** and **34** were synthesized as free thiols.

Comparison to the SAR for ColH inhibition

Interestingly, the here reported SAR shows an inverse activity profile of the *N*-aryl mercaptoacetamides compared to ColH. We previously reported polar, hydrogen bond-accepting substituents, especially in *para*-position to the aniline function, to be most potent for ColH inhibition.[35] Contrary to that, oxygen-containing compounds like e.g. the methoxy-derivatives **11**, **15**, **23** and **32** showed considerably weaker LasB inhibition compared to their halogen-substituted analogs. Strikingly, our best ColH inhibitor **1** is one of the weakest inhibitors described in this study. The position of the substituent substantially affects inhibition of ColH but not of LasB.

Confirmation of Thiols as Active Compounds.

As previously described[35], thiocarbamates are rapidly cleaved to the corresponding free thiols in aqueous buffers (Figure 4, A). Consequently, to confirm that the observed weaker activity on LasB compared to clostridial collagenases was not due to slower hydrolysis in LasB assay buffer, we performed the recently reported LC-MS-based stability test. Fast hydrolysis of **17** in 50 mM Tris pH 7.2 was observed with a thiocarbamate half-life of 3.7 ± 0.1 min (Figure 4, B). A third component was formed which is most likely the disulfide oxidation product. Compound hydrolysis proceeded faster than described for ColH assay at 22.5 °C[35], indicating temperature dependence of hydrolysis. Additionally, we found the same *in vitro* activity of selected thiols compared to their prodrugs,

confirming the results from the LC-MS assay that compound activation occurs within the pre-incubation time of our assay (Figure 4, C and Figure 5). Unlike thiols, which can be oxidized to disulfides[43], these thiocarbamate prodrugs have the advantage of being stable toward oxidation. As expected, the inactivity of dithiocarbamates **75-82** (Table S1) could be explained by their stability toward hydrolysis (Figure S2).

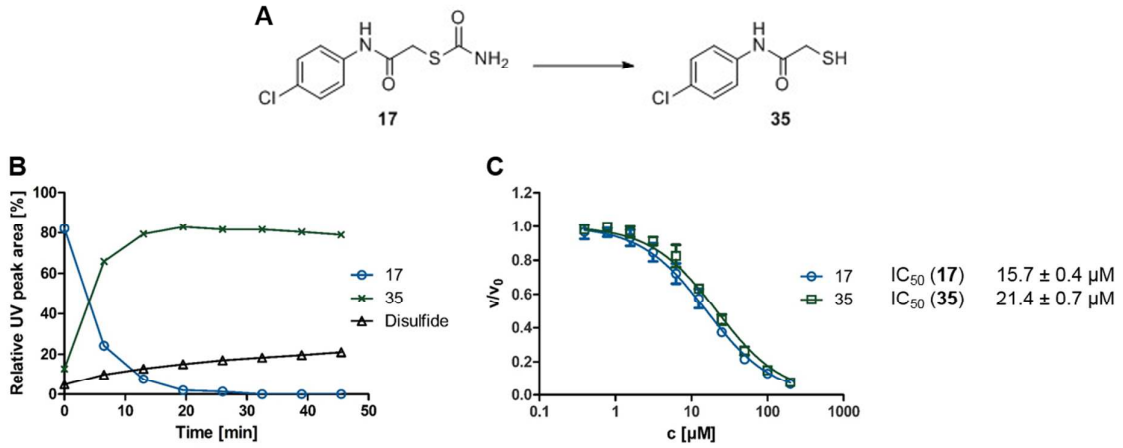

Figure 4. (A) Conversion of thiocarbamate **17** into corresponding free thiol **35**. (B) LC-MS stability assay showing fast hydrolysis of **17** into **35** in 50 mM Tris pH 7.2 (10% methanol) at 37 °C. (C) *In vitro* results for **17** and **35** are in accordance with the LC-MS results.

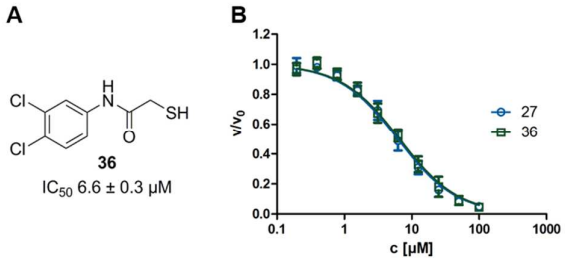

Figure 5. (A) Structure of thiol **36.** (B) FRET assay results for **36** and prodrug **27**. Non-linear regression was performed with the Hill Slope constrained to 1.

Binding Mode of Compound 36 to LasB.

To elucidate the binding mode of the *N*-aryl mercaptoacetamides to LasB we co-crystallized compound **27**, with LasB purified from *Pseudomonas aeruginosa* PA14 culture supernatant. The putative LasB-**27** complex crystallized in space group $P2_1$ and crystals diffracted to 1.3 Å resolution (Figure 6). The structure was solved by molecular replacement using the published LasB apo structure (PDB ID 1EZM) as a search model. Full details of the data collection and refinement statistics can be found in Table S2.

Hydrolysis of **27** to **36** was expected from the stability tests and from the *in vitro* assay using the corresponding thiol **36** and indeed there was no electron density for the thiocarbamate group observed. These observations confirm that the prodrug moiety does not contribute to the inhibitory activity. To our surprise, instead of one molecule, the active site of LasB contained unambiguous electron density for two molecules of **36**, arranged in an antiparallel fashion (hereafter referred to as $\mathbf{36}^{A}$ and $\mathbf{36}^{B}$). In the LasB apo structure, the active-site zinc ion is coordinated by the side-chains of His140, His144 and Glu164 as well as one water molecule. The free thiol of $\mathbf{36}^{A}$ displaces the water molecule to complete the tetrahedral coordination sphere (sulfur – zinc distance 2.3 Å). The carbonyl oxygen of $\mathbf{36}^{A}$ forms a bidentate hydrogen bond with Arg198 in the S1′ binding site (2.2 Å / 2.3 Å), while the side-chain of His223 forms a hydrogen bond with the thiol and amide nitrogen (2.4 Å / 3.5 Å). The amide nitrogen of the second molecule hydrogen bonds with Asn112 in the edge strand (2.0 Å), while its aromatic core lies in the lipophilic S2′ binding pocket. The tolerance of substitution at different positions without crucial changes in activity can be explained by the relatively large size of the binding site in comparison to the rather narrow binding pocket of ColH. Calculations performed with Molecular Operating Environment (MOE) software[44] enabled us to determine differences in the acidity of the thiol groups: Zinc coordination significantly increased thiol acidity, reducing the pk_a value from 9.0 in solution to 4.0. These results indicate full ionization of this sulfur atom when bound to the active site. By contrast, no significant change in the acidity of the non-zinc bound thiol could be determined, indicating a protonated state of this sulfur atom. It appears probable that binding of $\mathbf{36}^{A}$ is required for $\mathbf{36}^{B}$ to bind to the protein by providing a hydrophobic surface anchored to the active-site zinc ion $\mathbf{36}^{B}$ can interact with. Regarding the Hill Slope of 1 in the *in vitro* assay for **36** (Figure 5, B), it seems that only one binding event is necessary for full inhibition. This indicates that a second molecule might not be required for the activity of the compound and its absence in solution cannot be excluded.

Elastase belongs to the M4 family of peptidases, showing high similarity to thermolysin from *Bacillus thermoproteolyticus*.[27] Its LasB C-terminal domain is composed mostly of α-helices, while the N-terminal domain is formed predominantly by antiparallel β-sheets. The active site cleft is positioned within the hinge-region in between the two domains.[17] Interestingly, binding of $\mathbf{36}^{A}$ and $\mathbf{36}^{B}$ does not lead to a closure of the active site cleft as it has been reported after binding of phosphoramidon[45] and another peptidic inhibitor.[46] In fact, the open conformation observed in the apo structure is virtually unperturbed (C_α rmsd of just 0.24 over 290 residues, Figure S3). It seems likely that the antiparallel binding of two molecules of **36** prevents the active site from closing and thus allows addressing the enzyme in an open conformation. This offers a completely new avenue for the design of LasB inhibitors.

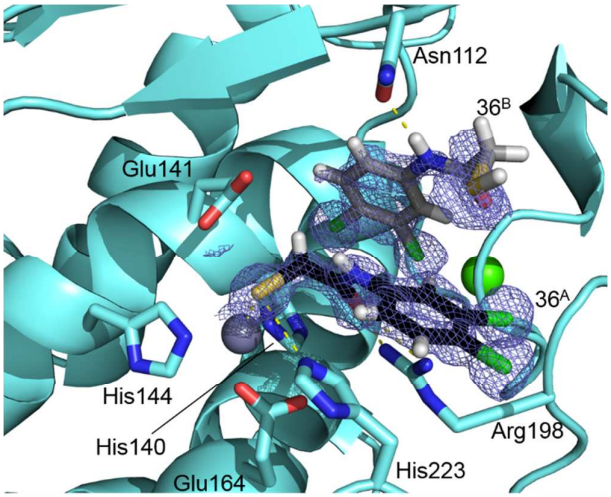

Figure 6. Structure of LasB in complex with **36**. Cartoon representations of LasB (cyan) in complex with **36** (black, grey). The difference electron density (F_o-F_c) contoured to 3σ with phases calculated from a model that was refined in the absence of **36** is shown as a yellow isomesh. The active-site zinc ion is shown as a grey, calcium ion as a green sphere. Residues involved in binding of $\mathbf{36}^{\mathbf{A}}$ and $\mathbf{36}^{\mathbf{B}}$ are shown as sticks.

In the work of Zhu et al., a primed binding mode of *N*-aryl mercaptoacetamides to the LasB active site was proposed based on docking studies.[34] We experimentally confirmed the inhibitor to be placed in the primed binding pocket. However, there are substantial differences in the orientation of the inhibitor, mainly owing to the presence of two molecules. The reported docking studies suggested additional chelation of the zinc atom by the carbonyl group of the inhibitor, which we demonstrated to hydrogen bond with Arg198. The proposed hydrogen bond between Asn112 and the amide nitrogen of the inhibitor is indeed present, yet it is formed by $\mathbf{36}^{\mathrm{B}}$ and not by the zinc chelating $\mathbf{36}^{\mathrm{A}}$.

Structure-based Optimization

Binding of a single molecule to the binding site instead of two might have an entropic benefit resulting in improved inhibition. Hence, we tried to replace the second, non-zinc chelating molecule and to grow the zinc-binding molecule deeper into the binding pocket, using the crystal structure of the LasB-**36** complex. Modeling approaches showed a benzyl group to be appropriate to fill the part of the binding pocket occupied by the aromatic core of the non-zinc binding molecule (Figure 7).

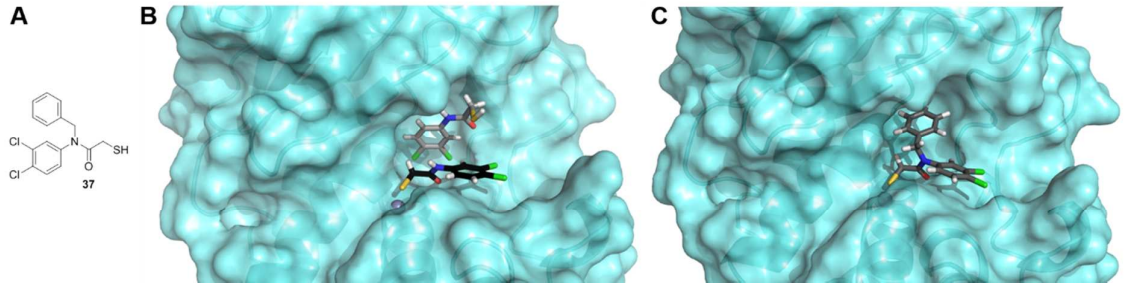

Figure 7. (A) Structure of **37**, the *N*-benzyl derivative of active thiol **36**. (B) Surface representation of LasB bound to two molecules of **27**. (C) Modeling of **37**, the *N*-benzyl derivative of the active thiol **36** based on the X-ray crystal structure.

A straightforward approach was used to synthesize *N*-benzyl derivatives of compound **27** (Scheme 1): *N*-benzyl substituted anilines **47-54** were obtained via reductive amination, using aniline **38** and a variety of benzaldehydes (**39-46**). Amide coupling with chloroacetyl chloride led to intermediates **55-62**. Replacement of the α-chlorine by a thiocyanate group was followed by hydrolysis to the respective thiocarbamates **63-70** using a mixture of concentrated sulfuric acid and acetic acid.[47]

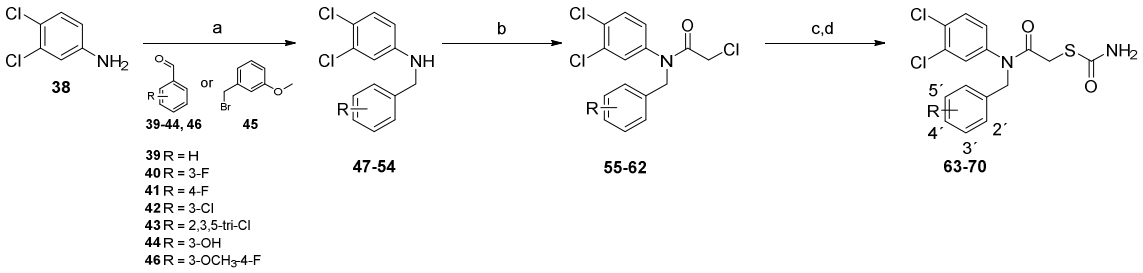

Scheme 1. Synthesis of *N*-benzyl mercaptoacetamides. Reagents and conditions: (a) sodium triacetoxyborohydride, DCM, RT, 20 h (**47-52**, **54**) or 3-methoxybenzylbromide, K_2CO_3, DMF, 120°C, 20 h (**53**); (b) chloroacetyl chloride, acetone, 0°C – r.t., 1.5 h; (c) ammonium thiocyanate, ethanol, 80°C, 2 h; (d) sulfuric acid, acetic acid, 0°C, 30 min

Introduction of a benzylic group at the position of the amide nitrogen of **27** led to an active compound with an IC_{50} of 20.4 ± 0.9 µM (**63**, Table 2). The activity was approximately threefold lower compared to the non-benzylated compound (Table 1). We introduced halogens at several positions of the benzyl group (**64-67**) to improve hydrophobic interactions with the lipophilic part of the binding pocket. The activity was slightly increased compared to **63**, however, with IC_{50}s in the two-digit micromolar range our compounds were still less active than **27**. The polar phenol and methoxyphenol derivatives **68** and **69** inhibited LasB in the same range as the halogenated compounds **64-67**, indicating that the lipophilic part of the binding pocket might not be reached. Combination of the 4′-fluorine of **65** and the 3′-methoxy group of **69** did not lead to an additive effect (**70**).

Table 2. Structure and LasB inhibition of *N*-substituted derivatives **63-74**.

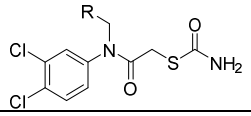

Cp.	R	IC_{50} (µM)
63	Ph	20.4 ± 0.9
64	3′-F-Ph	12.6 ± 0.4
65	4′-F-Ph	15.3 ± 0.6
66	3′-Cl-Ph	17.3 ± 0.8
67	2′,3′,5′-tri-Cl-Ph	15.9 ± 0.9
68	3′-OH-Ph	17.6 ± 0.6
69	3′-OCH_3-Ph	14.3 ± 0.6
70	3′-OCH_3-4′-F-Ph	18.3 ± 0.9
71	H	15.9 ± 0.7
72	*n*-C_4H_9	15.0 ± 0.5
73	*t*-C_4H_9	54.5 ± 2.3
74	C_6H_{11}	27.6 ± 1.4

Given that the activity could not be improved by introducing rigid aromatic functions, we investigated conformationally more flexible alkyl substituents. Synthesis was achieved following the same procedure (Scheme 1) using the respective alkyl aldehydes, giving compounds **71-74** (Table 2). Similar to the benzyl compounds **63-70**, introduction of alkyl substituents at the amide nitrogen led to a loss of activity, especially in case of the rather bulky neopentyl and cyclohexylmethyl substituents (**73** and **74**). Considering that replacement of the amide hydrogen by methyl group already resulted in a more than twofold loss of activity (**71**) we concluded that the hydrogen bond formed between Asn112 and the second molecule in the binding pocket plays an important role for compound binding.

To assess the impact of *N*-substitution on thiocarbamate half-life, the stability of **68** and **74** was analyzed. Again, we proved that thiocarbamates were cleaved rapidly, thus the reduced activity was not caused by slower compound activation in assay buffer (Figure S4).

Selectivity Toward Further Proteases.

MMPs are ubiquitously present in the human body, playing pivotal roles in the progress of various diseases, but also exerting beneficial effects on human health. The unselective inhibition of various MMPs was the reason for the failure of several protease inhibitors, while selectively inhibiting specific MMPs remains a challenging task in protease drug discovery.[48–53] Several bacterial protease inhibitors lacking MMP selectivity have been reported.[54–56] Thiol-based LasB inhibitors have been tested toward selected MMPs.[33,34] In this context, the inhibition of range of six MMPs with structural variation in

their S1′ binding pocket[57] (deep: MMP-3 and -14; intermediate: MMP-2 and -8; shallow: MMP-1 and -7) was analyzed for **27**. As we previously demonstrated for other *N*-aryl mercaptoacetamides[35], **27** did not inhibit this broad range of MMPs at concentrations up to 100 μM either (Figure S5).

In contrast to these antitargets, bacterial metallo-β-lactamases represent attractive additional targets, since cleavage of β-lactam antibiotics by these proteases is a crucial mechanism of antibiotic resistance.[58] Inhibition of metallo-β-lactamases by thiol-based inhibitors has been reported to restore the activity of β-lactam antibiotics.[59–62] To this end, we tested IMP-7, a metallo-β-lactamase present in clinical isolates of *P. aeruginosa* for *in vitro* inhibition by prodrug **27** and thiol **36**. Interestingly, the enzyme was found to be inhibited by **27** (1.16 ± 0.07 μM) as well as **36** (0.86 ± 0.06 μM).

Cytotoxicity Assays.

For a potential therapeutic application in humans, we analyzed the cytotoxicity of thiocarbamate **17** as well as thiols **35** and **36** toward two different human cell lines (Table 3). As described previously[35], the mercaptoacetamides had only a low cytotoxic effect on HEP G2 cells at a concentration as high as 100 μM. Likewise, the cytotoxic effect on HEK298 cells was also low at this high concentration.

Table 3. Cytotoxicity of **17**, **35** and **36** in HEP G2 and HEK298 cells.

Cp.	Concn [μM]	Reduction of viability [%]	
		HEP G2	HEK298
17	100	26 ± 16	51 ± 12
35	100	28 ± 12[a]	51 ± 4
36	100	25 ± 3	22 ± 5
Doxorubicin	1	50 ± 5[a]	49 ± 7
Rifampicin	100	29 ± 5[a]	19 ± 3
Batimastat	100	13 ± 7[a]	2 ± 2

[a]Values taken from Schönauer, Kany et al.[35]

***Galleria mellonella* Infection Model**

Stimulated by the promising *in vitro* results, the *in vivo* efficacy of our compounds was investigated. Infection models with *Galleria mellonella* larvae have previously been employed by us to assess novel treatment options for *Pseudomonas aeruginosa*-induced infections[63,64] and were reported to highly correlate with mouse models.[65] We analyzed the effect of prodrug **27** and active thiol **36** by co-injecting them with PA14. The larvae were challenged with PA14 concentrations corresponding to two times the LD_{50}.[65] Compared to PA14-infected larvae receiving no treatment, 2.5 nmol of **36** significantly increased the survival of *G. mellonella* from 43% to 72% after 65 hours (Figure 8). Notably, the survival rate was increased and not only the survival time, as reported for LasB inhibitors

in a *C. elegans* model.[34] However, administering the same concentration of thiocarbamate prodrug did not lead to a significant effect, indicating an insufficient release of the thiol in *G. mellonella* hemolymph. These findings prove the potential of LasB inhibition to effectively reduce *P. aeruginosa* pathogenicity.

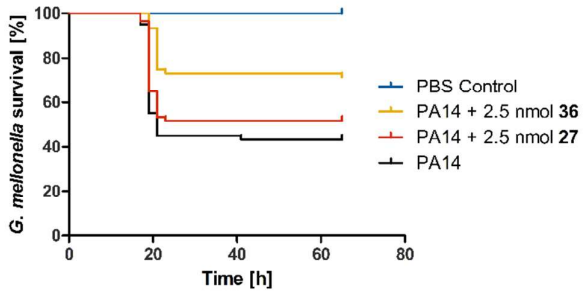

Figure 8. Survival curves for PA14-challenged *Galleria mellonella* larvae receiving treatment with 2.5 nmol **27** or **36** in comparison to larvae receiving treatment with PBS only. Curves represent results from at least three independent measurements. The survival rate was significantly higher for larvae treated with **36** ($p = 0.0003$, log-rank test) but not with **27**. The survival rate for larvae treated with the compounds in PBS was 100%.

CONCLUSION

In this study, a functional screening of a protease-inhibitor enriched library and a fragment library was performed using a well-established FRET assay, with the aim to expand the chemical space of LasB inhibitors. An LC-MS-based counterscreen was developed, allowing identification of false-positives. Only one real screening hit was identified, an *N*-aryl mercaptoacetamide. Compounds of this class are known to be inhibitors of LasB as well as of ColH from *C. histolyticum.* We analyzed the inhibition of further 35 derivatives of this class of fragment-like molecules. Interestingly, the SAR was inverse to the activity profile we discovered for ColH, allowing rational optimization of the compound class to selectively inhibit either LasB or ColH. The X-ray crystal structure of a LasB-inhibitor complex was solved, revealing a primed binding mode of two thiol molecules to the active site of the protease. Importantly, our results show that inhibitor binding does not necessarily lead to a closure of the binding pocket, as it has been described for thermolysin-like proteases. These findings pave the way for the development of novel LasB inhibitors targeting the open conformation of the enzyme, providing an important starting point for lead optimization. The structural information obtained by X-ray crystallography was used to grow the fragments by introducing benzyl or alkyl groups. These compounds indeed inhibited LasB, yet the activity was not improved. Supposably, the conformation of the *N*-substituted compounds is not ideal to replace the second inhibitor molecule in the binding pocket. With the β-lactamase IMP-7 we discovered an additional target of the *N*-aryl mercaptoacetamides, which is attractive for the development of novel anti-infectives. Furthermore, *in vivo* efficacy was demonstrated using a *Galleria mellonella* infection model. The survival rate of PA14-infected larvae was increased significantly when treated with our best thiol. Considering the

fragment-like character of our inhibitors, and the fact that they represent anti-virulence agents instead of traditional antibiotics, this is a remarkable effect. These results underline the potential of reducing bacterial pathogenicity to develop novel anti-bacterial drugs, which are urgently needed to combat antibiotic resistance. *N*-aryl mercaptoacetamides prove particularly interesting for the development of such drugs, since they display high selectivity toward human MMPs.

EXPERIMENTAL SECTION

Expression and Purification of LasB. *Pseudomonas aeruginosa* PA14 were grown in lysogeny broth medium for 72 h at 37 °C. Cells were removed by centrifugation (5000 rpm, 4 °C, 60 min) and the supernatant was filtered through a bottle-top-filter (0.20 µm). Purification was performed according to the method described by Morihara et al.[66] with few modifications. The precipitate formed by acetone treatment was dissolved in water and dialyzed against buffer A (20 mM Tris, pH 8.0). The dialyzed sample was then loaded onto a Hitrap Q HP column (GE Healthcare, Little Chalfont, UK) and washed back to baseline in buffer A, before being eluted with a gradient from buffer A into buffer A2 (20 mM Tris, pH 8.0, 1 M NaCl). The fractions with the strongest activity were pooled together (*in vitro* assay described below) and loaded onto a Superdex 200 gel filtration column (GE Healthcare) that was pre-equilibrates with buffer B (20 mM Tris, pH 8.0, 2 mM $CaCl_2$). Protein purity and activity was assessed by SDS-PAGE and in *vitro* inhibition assay.

***In vitro* Inhibition Assay.** For the initial screening, Elastase was purchased from Elastin Products Company (Owensville, MO, USA) or Merck (Darmstadt, Germany). Later, purified elastase prepared according to the procedure described above was used. The fluorogenic substrate 2-Aminobenzoyl-Ala-Gly-Leu-Ala-4-Nitrobenzylamide[36] was purchased from Peptides International (Louisville, KY, USA). Fluorescence intensity was measured for 60 min at 37°C in black 384-well microtiter plates (Greiner BioOne, Kremsmünster, Austria) using CLARIOstar microplate reader (BMG Labtech, Ortenberg, Germany) with an excitation wavelength of 340 ± 15 nm and an emission wavelength of 415 ± 20 nm. The assay was performed in a final volume of 50 µl assay buffer (50 mM Tris pH 7.2, 2.5 mM $CaCl_2$, 0.075% Pluronic F-127, 5% DMSO) containing LasB at a final concentration of 10 nM (commercial batch) or 0.3 nM (purified batch) and the substrate at 150 µM. Before substrate addition, compounds were pre-incubated with the enzyme for 15 min at 37°C. Experiments were performed in duplicates and repeated for at least two times. Blank controls without enzyme were performed. After blank subtraction, the slope of samples containing inhibitors (v) was divided by the slope of a simultaneously started uninhibited enzymatic reaction (v_0). IC_{50} values were determined with non-linear regression using GraphPad Prism 5 (Graph Pad Software, San Diego, CA, USA) and are given as mean values ± standard deviation (SD). The slope factor was constrained to 1.

LC-MS-based Readout for the FRET Assay. The FRET-based fluorescence assay was performed according to the procedure described above using 50 mM Tris pH 7.2. At the end of the measurement, the enzymatic reaction was stopped by adding formic acid at a final concentration of 2%. Simultaneously, amitryptiline were added as internal standard. The resulting mixture was diluted 1:10 in a mixture of 10% acetonitrile in MilliQ water containing 2% formic acid, resulting in a 10 µM amitryptiline concentration. The analyses were performed using a TF UltiMate 3000 binary RSLC UHPLC (Thermo Fisher, Dreieich, Germany) equipped with a degasser, a binary pump, an autosampler and a thermostated column compartment and a MWD, coupled to a TF TSQ Quantum Access Max mass spectrometer with heated electrospray ionization source (HESI-II). For gradient elution, an Accucore RP-MS column (150 × 2.1 mm, 2.6 µm, Thermo Fisher, Dreieich, Germany) was used with a mobile phase consisting of acetonitrile containing 1‰ formic acid (FA; v/v; eluent A) and water containing 1‰ FA (v/v; eluent B) at a flow rate of 400 µL/min under the following conditions: 0 – 0.9 min 10% A, 0.9 – 2.5 min 10 - 50% A, 2.5 – 5.5 min 50% - 70 % A, 5.5 – 6 min hold, 6 – 6.5 min 10% A, giving a total run time of 6.5 min. The injection volume was 10 µL. The divert valve was set to 1.6 min. The autosampler temperature was set to 6°C. The following MS conditions were used: electrospray ionization (ESI), positive mode, sheath gas, nitrogen at a flow rate of 35 arbitrary units; auxiliary gas, nitrogen at flow rate of 10 arbitrary units; vaporizer temperature, 50 °C; ion transfer capillary temperature, 270 °C; capillary offset, 15 V; spray voltage, 3000 V. The mass spectrometer was operated in the SIM mode with the following masses: **4** *m/z* 266.1 (tube lens offset 120 V), amitryptiline *m/z* 278.1 (tube lens offset 90 V), **5** m/z 337.0 (tube lens offset 120 V), **3** *m/z* 584.1 (tube lens offset 120 V) with a scan width of *m/z* 2.0 and a scan time of 0.1 s, respectively. Measurements were performed in duplicates and repeated for at least two times. Observed retention times were as follows: **4** 2.00 min, **5** 3.52 min, amitryptiline 4.02 min, **3** 4.37 min. MS-peak areas were determined using TF Xcalibur Software. Peak areas were normalized by ISTD peak area (giving A) and divided by the peak area of the respective ISTD normalized sample without inhibitor (A_0). IC_{50} values were determined using the method described above (GraphPad Prism 5 software).

LC-MS-based Stability Assay. The assay was performed as described previously[35] using 50 mM Tris pH 7.2 and a temperature of 37°C.

Screening Library. The protease inhibitor enriched screening library (ActiTarg-P) was purchased from TimTec (Newark, DE, USA). Fragments were obtained from the Maybridge Fragment Library (Maybridge, Altrincham, UK). Compounds were stored as DMSO stock solutions.

Chemistry. All reagents were used from commercial suppliers without further purification. Procedures were not optimized regarding yield. NMR spectra were recorded on a Bruker Fourier 300 (300 MHz) spectrometer. Chemical shifts are given in parts per million (ppm) and referenced against the residual proton, ^{1}H, or carbon, ^{13}C, resonances of the >99% deuterated solvents as internal reference. Coupling constants (*J*) are given in Hertz. Data are reported as follows: chemical shift,

multiplicity (s = singlet, d = doublet, t = triplet, m = multiplet, br = broad and combinations of these) coupling constants and integration. Mass spectrometry was performed on a SpectraSystems-MSQ LCMS system (Thermo Fisher, Dreieich, Germany). Flash chromatography was performed using the automated flash chromatography system CombiFlash Rf+ (Teledyne Isco, Lincoln, NE, USA) equipped with RediSepRf silica columns (Axel Semrau, Sprockhövel Germany) or Chromabond Flash C18 columns (Macherey-Nagel, Düren, Germany). Purity of compounds synthesized by us was determined by LCMS using the area percentage method on the UV trace recorded at a wavelength of 254 nm and found to be >95%. Thiols and thiocarbamates were synthesized according to the procedures described previously.[35] *N*-benzyl and *N*-aryl mercaptoacetamides were synthesized according to Scheme 1 and Scheme S2 using General Procedures 1-3 as described in more detail in the Supporting Information.

Human MMP Inhibition Assay. The catalytic domains of MMP-1, -2, -3, -7, -8 and -14 along with the SensoLyte 520 Generic MMP Activity Kit were purchased from AnaSpec (Fremont, CA, USA). The assay was performed as described previously using Batimastat as a positive control[35], according to the guidelines of the manufacturer.

β-lactamase Inhibition Assay. Activity assays for IMP-7 were carried out, as described by Klingler et al.[60] Final protein concentrations of 0.1 nM in a 50 mM HEPES buffer (pH 7.5, 0.01 % Triton X-100). Substrate (Fluorocillin™ (Invitrogen, Darmstadt, Germany) was dissolved in assay buffer to a final concentration of 888 nM. Test compounds were dissolved and pre-diluted in DMSO (final concentration: 1 %). In a black polystyrol 96-well plate (Corning) an amount of 1 µL of the respective inhibitor solution at different concentrations was incubated with 89 µL of IMP-7 containing buffer for 30 minutes at room temperature. 10 µL of substrate solution was added. The readout of the emitted fluorescence was started immediately (45 s for 30 cycles) using a Tecan Infinite F200Pro (Tecan Group Ltd; excitation at 495 nm and emission at 525 nm). Blank controls were performed without enzyme. Positive controls were performed with enzyme but without inhibitor. The inhibitory activity of each test compound was measured in three independent experiments. For calculation of IC_{50} values, data obtained from measurements with eight different inhibitor concentrations were used. For the evaluation of the sigmoidal dose response equation (variable slope with four parameters) GraphPad Prism 5 (*GraphPad Software,* La Jolla, CA, USA) was used.

Cytotoxicity Assays. Hep G2 or HEK298 cells (2×10^5 cells per well) were seeded in 24-well, flat-bottomed plates. Culturing of cells, incubations and OD measurements were performed as described previously[67] with small modifications. 24 h after seeding the cells the incubation was started by the addition of compounds in a final DMSO concentration of 1 %. The living cell mass was determined after 48 h. At least two independent measurements were performed for each compound.

***Galleria mellonella* Virulence Assay.** The virulence assay was performed as described by Lu, Maurer et al[63] with some modifications: *Galleria mellonella* larvae (TruLarv™) were purchased from

BioSystems Technology (Exeter, United Kingdom). Injections were performed using a LA120 syringe pump (Landgraf Laborsysteme, Langenhagen, Germany) equipped with 1 ml Injekt-F tuberculin syringes (B. Braun, Melsungen, Germany) and Sterican 0.30 x 12 mm, 30G x 1½ needles (B. Braun). The following treatment conditions were applied: (a) sterile PBS solution, (b) PA14 suspension, (c) 2.5 nmol **27** in "b", (d) 2.5 nmol **36** in "b", (e) 2.5 nmol **27** in "a", (f) 1.25 nmol **36** in "a". Samples a-e contained 1% DMSO and f 0.5%. For each treatment, data from at least three independent measurements were combined.

X-ray Crystallography. LasB was concentrated to 10 -12 mg/mL and mixed with inhibitor **27** at a final concentration of 1 mM. Complex crystals were grown by the sitting drop method using a reservoir solution containing 0.2 M Magnesium Chloride and 30% (w/v) PEG 3350. Crystals were cryoprotected in glycerol and diffraction data was collected from single crystals at 100 K at beamline ID23-2 (ESRF) at a wavelength of 0.873 Å. Data was processed using Xia2[68] and the structure solved using PHASER[69] molecular replacement with *Pseudomonas aeruginosa* elastase (PAE, PDB ID 1EZM) as a search model. The solution was manually rebuilt with COOT[70] and refined using PHENIX[71] and Refmac5[72]. The final refined structure of LasB in complex with compound **27** was deposited in the Protein Data Bank (PDB) as entry 6F8B.

Molecular Modeling. Molecular modeling was performed with Molecular Operating Environment 2015.10 (MOE) software (Chemical Computing Group, Montreal, Canada) using standard parameters. In the co-crystal structure of LasB and **36,** inhibitor molecule $\mathbf{36^B}$ was removed and $\mathbf{36^A}$ was grown using the Builder function. The final structure was energy-minimized using the QuickPrep function. AMBER10:EHT was used as a force field.

ASSOCIATED CONTENT

Supporting Information. Supporting Table T1-T2 and Figures S1-S4, giving structures and stability data of inactive compounds, X-ray data collection and refinement statistics, FRET and LC-MS results for phosphoramidon, stability data for **68** and **74**, MMP inhibition assay, experimental procedures and spectral data for synthetic compounds

AUTHOR CONTRIBUTIONS

⊥A.M.K. and A.S. contributed equally.

ACKNOWLEDGEMENTS

We thank Jeannine Jung, Simone Amann, Tabea Schramm and Lilia Weizel for technical support, Dr. Jens Eberhard and Dr. Giuseppe Allegretta for help with the establishment of the LC-MS assay, Dr. Teresa Röhrig for support with the *G. mellonella* assay and Dr. Martin Empting for help with molecular modeling. E.P. thanks German Research Foundation (DFG, Heisenberg-Professur PR1405/4-1) for financial support.

References

1 World Health Organization (2017) *Antibacterial Agents in Clinical Development. An analysis of the antibacterial clinical development pipeline, including tuberculosis.* World Health Organization, Geneva.

2 Taubes, G. (2008) The bacteria fight back. *Science.* 321, 356–361. DOI: 10.1126/science.321.5887.356.

3 Hancock, R. E. W., Speert, D. P. (2000) Antibiotic resistance in Pseudomonas aeruginosa. Mechanisms and impact on treatment. *Drug Resist. Updat.* 3, 247–255. DOI: 10.1054/drup.2000.0152.

4 Sordé, R., Pahissa, A., Rello, J. (2011) Management of refractory Pseudomonas aeruginosa infection in cystic fibrosis. *Infect Drug. Resist.* 4, 31–41. DOI: 10.2147/IDR.S16263.

5 Mesaros, N., Nordmann, P., Plésiat, P., Roussel-Delvallez, M., van Eldere, J., Glupczynski, Y., van Laethem, Y., Jacobs, F., Lebecque, P., Malfroot, A., Tulkens, P. M., van Bambeke, F. (2007) Pseudomonas aeruginosa. Resistance and therapeutic options at the turn of the new millennium. *Clin. Microbiol. Infect.* 13, 560–578. DOI: 10.1111/j.1469-0691.2007.01681.x.

6 Cooper, M. A., Shlaes, D. (2011) Fix the antibiotics pipeline. *Nature.* 472, 32. DOI: 10.1038/472032a.

7 Dickey, S. W., Cheung, G. Y. C., Otto, M. (2017) Different drugs for bad bugs. Antivirulence strategies in the age of antibiotic resistance. *Nat. Rev. Drug Discov.* 16, 457–471. DOI: 10.1038/nrd.2017.23.

8 Heras, B., Scanlon, M. J., Martin, J. L. (2015) Targeting virulence not viability in the search for future antibacterials. *Br. J. Clin. Pharmacol.* 79, 208–215. DOI: 10.1111/bcp.12356.

9 Lewis, K. (2013) Platforms for antibiotic discovery. *Nat. Rev. Drug Discov.* 12, 371–387. DOI: 10.1038/nrd3975.

10 Rasko, D. A., Sperandio, V. (2010) Anti-virulence strategies to combat bacteria-mediated disease. *Nat. Rev. Drug Discov.* 9, 117–128. DOI: 10.1038/nrd3013.

11 Strateva, T., Mitov, I. (2011) Contribution of an arsenal of virulence factors to pathogenesis of Pseudomonas aeruginosa infections. *Ann. Microbiol.* 61, 717–732. DOI: 10.1007/s13213-011-0273-y.

12 Wagner, S., Sommer, R., Hinsberger, S., Lu, C., Hartmann, R. W., Empting, M., Titz, A. (2016) Novel Strategies for the Treatment of Pseudomonas aeruginosa Infections. *J. Med. Chem.* 59, 5929–5969. DOI: 10.1021/acs.jmedchem.5b01698.

13 Storz, M. P., Maurer, C. K., Zimmer, C., Wagner, N., Brengel, C., Jong, J. C. de, Lucas, S., Müsken, M., Häussler, S., Steinbach, A., Hartmann, R. W. (2012) Validation of PqsD as an anti-biofilm target in Pseudomonas aeruginosa by development of small-molecule inhibitors. *J. Am. Chem. Soc.* 134, 16143–16146. DOI: 10.1021/ja3072397.

14 Kamal, A. A. M., Maurer, C. K., Allegretta, G., Haupenthal, J., Empting, M., Hartmann, R. W. (2017) Quorum Sensing Inhibitors as Pathoblockers for Pseudomonas aeruginosa Infections: A New Concept in Anti-Infective Drug Discovery. In Topics in Medicinal Chemistry, pp 1-26, Springer, Berlin, Heidelberg.

15 Wretlind, B., Pavlovskis, O. R. (1983) Pseudomonas aeruginosa elastase and its role in Pseudomonas infections. *Rev. Infect. Dis.* 5 Suppl 5, S998-1004.

16 Morihara, K. (1964) Production of elastase and proteinase by Pseudomonas aeruginosa. *J. Bacteriol.* 88, 745–757.

17 Thayer, M. M., Flaherty, K. M., Mckay, D. B. (1991) Three-dimensional structure of the elastase of Pseudomonas aeruginosa at 1.5-A resolution. *J. Biol. Chem.* 266, 2864–2871.

18 Heck, L. W., Morihara, K., McRae, W. B., Miller, E. J. (1986) Specific cleavage of human type III and IV collagens by Pseudomonas aeruginosa elastase. *Infect. Immun.* 51, 115–118.

19 Golovkine, G., Faudry, E., Bouillot, S., Voulhoux, R., Attrée, I., Huber, P. (2014) VE-cadherin cleavage by LasB protease from Pseudomonas aeruginosa facilitates type III secretion system toxicity in endothelial cells. *PLoS Pathog.* 10, e1003939. DOI: 10.1371/journal.ppat.1003939.

20 Azghani, A. O. (1996) Pseudomonas aeruginosa and epithelial permeability. Role of virulence factors elastase and exotoxin A. *Am. J. Respir. Cell. Mol. Biol.* 15, 132–140. DOI: 10.1165/ajrcmb.15.1.8679217.

21 Holder, I. A., Wheeler, R. (1984) Experimental studies of the pathogenesis of infections owing to Pseudomonas aeruginosa. Elastase, an IgG protease. *Can. J. Microbiol.* 30, 1118–1124.

22 Parmely, M., Gale, A., Clabaugh, M., Horvat, R., Zhou, W. W. (1990) Proteolytic inactivation of cytokines by Pseudomonas aeruginosa. *Infect. Immun.* 58, 3009–3014.

23 Mariencheck, W. I., Alcorn, J. F., Palmer, S. M., Wright, J. R. (2003) Pseudomonas aeruginosa elastase degrades surfactant proteins A and D. *Am. J. Respir. Cell. Mol. Biol.* 28, 528–537. DOI: 10.1165/rcmb.2002-0141OC.

24 Schmidtchen, A., Holst, E., Tapper, H., Björck, L. (2003) Elastase-producing Pseudomonas aeruginosa degrade plasma proteins and extracellular products of human skin and fibroblasts, and inhibit fibroblast growth. *Microb. Pathog.* 34, 47–55. DOI: 10.1016/S0882-4010(02)00197-3.

25 Dulon, S., Leduc, D., Cottrell, G. S., D'Alayer, J., Hansen, K. K., Bunnett, N. W., Hollenberg, M. D., Pidard, D., Chignard, M. (2005) Pseudomonas aeruginosa elastase disables proteinase-activated receptor 2 in respiratory epithelial cells. *Am. J. Respir. Cell. Mol. Biol.* 32, 411–419. DOI: 10.1165/rcmb.2004-0274OC.

26 Graef, F., Vukosavljevic, B., Michel, J.-P., Wirth, M., Ries, O., Rossi, C. de, Windbergs, M., Rosilio, V., Ducho, C., Gordon, S., Lehr, C.-M. (2016) The bacterial cell envelope as delimiter of anti-infective bioavailability - An in vitro permeation model of the Gram-negative bacterial inner membrane. *J. Control. Release.* 243, 214–224. DOI: 10.1016/j.jconrel.2016.10.018.

27 Adekoya, O. A., Sylte, I. (2009) The thermolysin family (M4) of enzymes. Therapeutic and biotechnological potential. *Chem. Biol. Drug Des.* 73, 7–16. DOI: 10.1111/j.1747-0285.2008.00757.x.

28 Holland, D. R., Tronrud, D. E., Pley, H. W., Flaherty, K. M., Stark, W., Jansonius, J. N., Mckay, D. B., Matthews, B. W. (1992) Structural comparison suggests that thermolysin and related neutral proteases undergo hinge-bending motion during catalysis. *Biochemistry.* 31, 11310–11316.

29 Adekoya, O. A., Sjøli, S., Wuxiuer, Y., Bilto, I., Marques, S. M., Santos, M. A., Nuti, E., Cercignani, G., Rossello, A., Winberg, J.-O., Sylte, I. (2015) Inhibition of pseudolysin and thermolysin by hydroxamate-based MMP inhibitors. *Eur. J. Med. Chem.* 89, 340–348. DOI: 10.1016/j.ejmech.2014.10.009.

30 Fullagar, J. L., Garner, A. L., Struss, A. K., Day, J. A., Martin, D. P., Yu, J., Cai, X., Janda, K. D., Cohen, S. M. (2013) Antagonism of a zinc metalloprotease using a unique metal-chelating scaffold. Tropolones as inhibitors of P. aeruginosa elastase. *Chem. Commun. (Camb).* 49, 3197–3199. DOI: 10.1039/c3cc41191e.

31 Burns, F. R., Paterson, C. A., Gray, R. D., Wells, J. T. (1990) Inhibition of Pseudomonas aeruginosa elastase and Pseudomonas keratitis using a thiol-based peptide. *Antimicrob. Agents. Chemother.* 34, 2065–2069.

32 Kessler, E., Israel, M., Landshman, N., Chechick, A., Blumberg, S. (1982) In vitro inhibition of Pseudomonas aeruginosa elastase by metal-chelating peptide derivatives. *Infect. Immun.* 38, 716–723.

33 Cathcart, G. R. A., Quinn, D., Greer, B., Harriott, P., Lynas, J. F., Gilmore, B. F., Walker, B. (2011) Novel inhibitors of the Pseudomonas aeruginosa virulence factor LasB. A potential therapeutic approach for the attenuation of virulence mechanisms in pseudomonal infection. *Antimicrob. Agents. Chemother.* 55, 2670–2678. DOI: 10.1128/AAC.00776-10.

34 Zhu, J., Cai, X., Harris, T. L., Gooyit, M., Wood, M., Lardy, M., Janda, K. D. (2015) Disarming Pseudomonas aeruginosa virulence factor LasB by leveraging a Caenorhabditis elegans infection model. *Chem. Biol.* 22, 483–491. DOI: 10.1016/j.chembiol.2015.03.012.

35 Schönauer, E., Kany, A. M., Haupenthal, J., Hüsecken, K., Hoppe, I. J., Voos, K., Yahiaoui, S., Elsässer, B., Ducho, C., Brandstetter, H., Hartmann, R. W. (2017) Discovery of a Potent Inhibitor Class with High Selectivity toward Clostridial Collagenases. *J. Am. Chem. Soc.* 139, 12696–12703. DOI: 10.1021/jacs.7b06935.

36 Nishino, N., Powers, J. C. (1980) Pseudomonas aeruginosa elastase. Development of a new substrate, inhibitors, and an affinity ligand. *J. Biol. Chem.* 255, 3482–3486.

37 Baell, J. B., Holloway, G. A. (2010) New substructure filters for removal of pan assay interference compounds (PAINS) from screening libraries and for their exclusion in bioassays. *J. Med. Chem.* 53, 2719–2740. DOI: 10.1021/jm901137j.

38 Lakowicz, J. R. (2010) *Principles of Fluorescence Spectroscopy,* 3. ed., Springer, New York, NY.

39 Kongkamnerd, J., Milani, A., Cattoli, G., Terregino, C., Capua, I., Beneduce, L., Gallotta, A., Pengo, P., Fassina, G., Monthakantirat, O., Umehara, K., De-Eknamkul, W., Miertus, S. (2011) The quenching effect of flavonoids on 4-methylumbelliferone, a potential pitfall in fluorimetric neuraminidase inhibition assays. *J. Biomol. Screen.* 16, 755–764. DOI: 10.1177/1087057111409221.

40 Shapiro, A. B., Walkup, G. K., Keating, T. A. (2009) Correction for interference by test samples in high-throughput assays. *J. Biomol. Screen.* 14, 1008–1016. DOI: 10.1177/1087057109341768.

41 Morihara, K., Tsuzuki, H. (1971) Comparative study of various neutral proteinases from microorganisms. Specificity with oligopeptides. *Arch. Biochem. Biophys.* 146, 291–296.

42 Morihara, K., Tsuzuki, H. (1978) Phosphoramidon as an inhibitor of elastase from Pseudomonas aeruginosa. *Jpn. J. Exp. Med.* 48, 81–84.

43 Pramar, Y., Das Gupta, V., Bethea, C. (1992) Stability of captopril in some aqueous systems. *J. Clin. Pharm. Ther.* 17, 185–189.

44 Labute, P. (2009) Protonate3D. Assignment of ionization states and hydrogen coordinates to macromolecular structures. *Proteins.* 75, 187–205. DOI: 10.1002/prot.22234.

45 Mckay, D. B., Overgaard, M. T. (2009) Pseudomonas aeruginosa elastase with phosphoramidon. DOI: 10.2210/pdb3dbk/pdb.

46 Bitto, E., Mckay, D. B. (2004) Elastase of Pseudomonas aeruginosa with an inhibitor. DOI: 10.2210/pdb1u4g/pdb.

47 Kim, Y.-G., Lim, H. N., Lee, K.-J. (2009) A new route to allyl thiols and allyl thiocarbamates from Baylis-Hillman adducts. *J. Heterocyclic Chem.* 46, 23–27. DOI: 10.1002/jhet.3.

48 Cathcart, J., Pulkoski-Gross, A., Cao, J. (2015) Targeting Matrix Metalloproteinases in Cancer. Bringing New Life to Old Ideas. *Genes Dis.* 2, 26–34. DOI: 10.1016/j.gendis.2014.12.002.

49 Dufour, A., Overall, C. M. (2013) Missing the target. Matrix metalloproteinase antitargets in inflammation and cancer. *Trends Pharmacol. Sci.* 34, 233–242. DOI: 10.1016/j.tips.2013.02.004.

50 Overall, C. M., López-Otín, C. (2002) Strategies for MMP inhibition in cancer. Innovations for the post-trial era. *Nat. Rev. Cancer.* 2, 657–672. DOI: 10.1038/nrc884.

51 Sbardella, D., Fasciglione, G. F., Gioia, M., Ciaccio, C., Tundo, G. R., Marini, S., Coletta, M. (2012) Human matrix metalloproteinases. An ubiquitarian class of enzymes involved in several pathological processes. *Mol. Aspects Med.* 33, 119–208. DOI: 10.1016/j.mam.2011.10.015.

52 Turk, B. (2006) Targeting proteases. Successes, failures and future prospects. *Nat. Rev. Drug Discov.* 5, 785–799. DOI: 10.1038/nrd2092.

53 Vandenbroucke, R. E., Libert, C. (2014) Is there new hope for therapeutic matrix metalloproteinase inhibition? *Nat. Rev. Drug Discov.* 13, 904–927. DOI: 10.1038/nrd4390.

54 Ilies, M., Banciu, M. D., Scozzafava, A., Ilies, M. A., Caproiu, M. T., Supuran, C. T. (2003) Protease inhibitors. Synthesis of bacterial collagenase and matrix metalloproteinase inhibitors incorporating arylsulfonylureido and 5-dibenzo-suberenyl/suberyl moieties. *Bioorg. Med. Chem.* 11, 2227–2239. DOI: 10.1016/S0968-0896(03)00113-5.

55 Scozzafava, A., Supuran, C. T. (2002) Protease inhibitors. Synthesis of matrix metalloproteinase and bacterial collagenase inhibitors incorporating 5-amino-2-mercapto-1,3,4-thiadiazole zinc binding functions. *Bioorg. Med. Chem. Lett.* 12, 2667–2672.

56 Sjøli, S., Nuti, E., Camodeca, C., Bilto, I., Rossello, A., Winberg, J.-O., Sylte, I., Adekoya, O. A. (2016) Synthesis, experimental evaluation and molecular modelling of hydroxamate derivatives as zinc metalloproteinase inhibitors. *Eur. J. Med. Chem.* 108, 141–153. DOI: 10.1016/j.ejmech.2015.11.019.

57 Park, H. I., Jin, Y., Hurst, D. R., Monroe, C. A., Lee, S., Schwartz, M. A., Sang, Q.-X. A. (2003) The intermediate S1' pocket of the endometase/matrilysin-2 active site revealed by enzyme inhibition kinetic studies, protein sequence analyses, and homology modeling. *J. Biol. Chem.* 278, 51646–51653. DOI: 10.1074/jbc.M310109200.

58 Bush, K., Fisher, J. F. (2011) Epidemiological expansion, structural studies, and clinical challenges of new β-lactamases from gram-negative bacteria. *Annu. Rev. Microbiol.* 65, 455–478. DOI: 10.1146/annurev-micro-090110-102911.

59 Buynak, J. D., Chen, H., Vogeti, L., Gadhachanda, V. R., Buchanan, C. A., Palzkill, T., Shaw, R. W., Spencer, J., Walsh, T. R. (2004) Penicillin-derived inhibitors that simultaneously target both metallo- and serine-beta-lactamases. *Bioorg. Med. Chem. Lett.* 14, 1299–1304. DOI: 10.1016/j.bmcl.2003.12.037.

60 Klingler, F.-M., Wichelhaus, T. A., Frank, D., Cuesta-Bernal, J., El-Delik, J., Müller, H. F., Sjuts, H., Göttig, S., Koenigs, A., Pos, K. M., Pogoryelov, D., Proschak, E. (2015) Approved Drugs Containing Thiols as Inhibitors of Metallo-β-lactamases. Strategy To Combat Multidrug-Resistant Bacteria. *J. Med. Chem.* 58, 3626–3630. DOI: 10.1021/jm501844d.

61 Tehrani, K. H. M. E., Martin, N. I. (2017) Thiol-Containing Metallo-β-Lactamase Inhibitors Resensitize Resistant Gram-Negative Bacteria to Meropenem. *ACS Infect. Dis.* 3, 711–717. DOI: 10.1021/acsinfecdis.7b00094.

62 Büttner, D., Kramer, J. S., Klingler, F.-M., Wittmann, S. K., Hartmann, M. R., Kurz, C. G., Kohnhäuser, D., Weizel, L., Brüggerhoff, A., Frank, D., Steinhilber, D., Wichelhaus, T. A., Pogoryelov, D., Proschak, E. (2017) Challenges in the Development of a Thiol-Based Broad-Spectrum Inhibitor for Metallo-β-Lactamases. *ACS Infect. Dis. DOI:* 10.1021/acsinfecdis.7b00129.

63 Lu, C., Maurer, C. K., Kirsch, B., Steinbach, A., Hartmann, R. W. (2014) Overcoming the unexpected functional inversion of a PqsR antagonist in Pseudomonas aeruginosa. An in vivo potent antivirulence agent targeting pqs quorum sensing. *Angew. Chem. Int. Ed. Engl.* 53, 1109–1112. DOI: 10.1002/anie.201307547.

64 Thomann, A., Mello Martins, A. G. G. de, Brengel, C., Empting, M., Hartmann, R. W. (2016) Application of Dual Inhibition Concept within Looped Autoregulatory Systems toward Antivirulence Agents against Pseudomonas aeruginosa Infections. *ACS Chem. Biol.* 11, 1279–1286. DOI: 10.1021/acschembio.6b00117.

65 Jander, G., Rahme, L. G., Ausubel, F. M. (2000) Positive correlation between virulence of Pseudomonas aeruginosa mutants in mice and insects. *J. Bacteriol.* 182, 3843–3845.

66 Morihara, K., Tsuzuki, H., Oka, T., Inoue, H., Ebata, M. (1965) Pseudomonas aeruginosa elastase: isolation, crystallization, and preliminary characterization. *J. Biol. Chem.* 240, 3295–3304.

67 Haupenthal, J., Baehr, C., Zeuzem, S., Piiper, A. (2007) RNAse A-like enzymes in serum inhibit the anti-neoplastic activity of siRNA targeting polo-like kinase 1. *Int. J. Cancer.* 121, 206–210. DOI: 10.1002/ijc.22665.

68 Winter, G. (2010) xia2. An expert system for macromolecular crystallography data reduction. *J. Appl. Crystallogr.* 43, 186–190. DOI: 10.1107/S0021889809045701.

69 McCoy, A. J., Grosse-Kunstleve, R. W., Adams, P. D., Winn, M. D., Storoni, L. C., Read, R. J. (2007) Phaser crystallographic software. *J. Appl. Crystallogr.* 40, 658–674. DOI: 10.1107/S0021889807021206.

70 Emsley, P., Lohkamp, B., Scott, W. G., Cowtan, K. (2010) Features and development of Coot. *Acta Cryst. D.* 66, 486–501. DOI: 10.1107/S0907444910007493.

71 Adams, P. D., Afonine, P. V., Bunkóczi, G., Chen, V. B., Davis, I. W., Echols, N., Headd, J. J., Hung, L.-W., Kapral, G. J., Grosse-Kunstleve, R. W., McCoy, A. J., Moriarty, N. W., Oeffner, R., Read, R. J., Richardson, D. C., Richardson, J. S., Terwilliger, T. C., Zwart, P. H. (2010) PHENIX. A comprehensive Python-based system for macromolecular structure solution. *Acta Cryst. D.* 66, 213–221. DOI: 10.1107/S0907444909052925.

72 Skubák, P., Murshudov, G. N., Pannu, N. S. (2004) Direct incorporation of experimental phase information in model refinement. *Acta Cryst. D.* 60, 2196–2201. DOI: 10.1107/S0907444904019079.

Table of contents artwork